SHOCK, Vol. 19, No. 6, pp. 582–587, 2003

SUPPRESSION OF PROTEIN KINASE Cα TRIGGERS APOPTOSIS THROUGH DOWN-REGULATION OF BCL-XL IN A RAT HEPATIC EPITHELIAL CELL LINE

Ya-Ching Hsieh, Hsiao-Ching Jao, Rei-Cheng Yang, Hseng-Kuang Hsu, and Chin Hsu

Department of Physiology, Kaohsiung Medical University, Kaohsiung, Taiwan

Received 22 Oct 2002; first review completed 5 Nov 2002; accepted in final form 30 Dec 2002

ABSTRACT—Inactivation of protein kinase C (PKC)α plays an important role in modulating hepatic failure and/or apoptosis during sepsis. To determine whether and how PKCα inactivation mediates the apoptosis, PKCα was suppressed by antisense treatment or transiently transfection in Clone-9 rat hepatic epithelial cell line. Apoptosis was evaluated by cell survival rate, poly-adenyl ribonuclease polymerase (PARP) cleavage, and terminal deoxynucleotidyl transferase-mediated deoxyuridine triphosphate-digoxigenin nick end labeling stain. The expressions of PKCα and Bcl-xL were quantified by Western blot analysis after antisense treatment. In the transfection studies, cells were co-transfected with green fluorescent protein cDNA as a transfection marker. The expressions of PKCα and Bcl-xL were detected by immunohistochemical staining with second antibody conjugated with Texas red. Apoptosis was evaluated by tetramethyl-rhodamine labeling of DNA strand breaks and immunostaining of 85-kDa fragment of PARP. The results showed that cytosolic and membrane-associated PKCα were decreased by 54.5% and 41.4%, respectively, after PKCα antisense treatment. The apoptotic incidence and percentage of PARP cleavage were significantly increased, whereas protein expression of Bcl-xL was decreased after PKCα-antisense treatment. In the transfection studies, the results showed that most of the cells expressing green fluorescent protein revealed less PKCα and Bcl-xL protein contents and more *in situ* PARP cleavage and DNA strand breaks. These findings indicated that decrease of PKCα declines the Bcl-xL content and leads to the vulnerability of apoptosis in hepatic epithelial cells. Taken together, our data provide evidence that suppression of PKCα plays a critical role in triggering caspase-dependent apoptosis, which may act through modulating the Bcl-xL expression.

KEYWORDS—PKCα, apoptosis, Bcl-xL, PARP

INTRODUCTION

Our previous work has shown that inactivation of protein kinase C (PKC) may play a critical role in modulating hepatic failure during sepsis (1). However, the participation of PKC in signal transduction pathways that regulate liver function is likely to be a complex process because PKC is a multigene family consisting of 11 closely related isoforms. Recently, we screened the changes of all isoforms in the liver during sepsis and found that alteration of PKCα is the most prominent one during sepsis (2). PKCα is essentially involved in maintaining cells in an antiapoptotic state such as glioma cell (3) and myoblast (4). Our recent result also showed that inactivation of PKCα was accompanied by reduction in Bcl-xL levels during sepsis that coincided with the appearance of apoptotic cell death as detected by outlet exposure of phosphatidylserine (5). However, despite these evidences, the causal relationship between PKCα and the downstream effectors that are involved in the hepatic apoptosis have not been identified. Accordingly, we design an *in vitro* system of PKCα suppression that was simulated by transient antisense treatment or transfected with an expression vector containing the cDNA for rat PKCα in the antisense orientation to identify the *in situ* alterations after PKCα suppression for a long duration. Then, caspase-activated PARP cleavage, apoptotic incidence, and expression of Bcl-xL, which is down-regulated by PKCα inactivation (3), were evaluated after PKCα suppression. In the present study, we demonstrated that inhibition of PKCα leads to a decrease in Bcl-xL protein content and induction of apoptosis.

MATERIALS AND METHODS

Inhibition of PKCα protein synthesis by antisense treatment

Clone 9 rat hepatic epithelial cells were pre-treated with 1 μM phorbol 12, 13-dibutyrate (PDBu) for 12 h until 70–80% confluent. This procedure removes greater than 90% of PKC protein from the cells (6). Then medium was replaced with F12 K to remove PDBu and incubated with 1 μM PKCα antisense for 6 h (7). Then, the cells were sampled for analysis of expressions of PKCα and Bcl-xL as well as apoptosis 18 h later.

Extraction and purification of PKCα

PKCα was extracted and partial purified by the method of Wise et al. (8) with modification. Cells were homogenized in 300 μL of buffer (25 mM Tris-Base; 2 mM EDTA; 10 mM EGTA, pH 7.46; 10 mM DTT; 150 mM sucrose; 1% protein enzyme inhibitor) and then centrifuged at 30,000 g for 15 min. The supernatant containing enzyme was used as cytosolic fraction. The resulting pellet was rehomogenized in buffer A containing 0.25% Triton X-100. The mixture was incubated for 15 min on ice followed by centrifugation at 30,000 g for 15 min and the resulting supernatant was used as enzyme of membrane-associated fraction.

Western analysis of PKCα isoform

Equal amount of sample (5 μg) was subjected to SDS-PAGE using a 7.5% running gel (9). Proteins were transferred onto polyvinylidene difluoride transfer membrane by electroblotting for 55 min (120 v). PKCα antibody (1:1000, Transductional Laboratory. Cat No. P16520) was incubated with the membrane for 1 h at room temperature. The membranes were washed in TBS-t and incubated with goat anti-mouse horseradish peroxidase antiserum (1:5000, Transduction Laboratory, cat no. M15345) for 1 h. Then, the membranes were detected by the ECL system.

Determination of cell survival rate

Cell survival was determined by trypan blue exclusion after treating cells with PKCα antisense oligonucleotides, and enumeration of viable cells using a hemocytometer.

Address reprint requests to Chin Hsu, Department of Physiology, Kaohsiung Medical University, Kaohsiung city, Taiwan.

This work was supported by NSC-90-2320-B-037-025 and NSC-91-2745-B-037-002 (Taiwan).

DOI: 10.1097/01.shk.0000065705.84144.ed

Terminal deoxynucleotidyl transferase-mediated deoxyuridine triphosphate-digoxigenin nick end labeling (TUNEL) staining

Cells were cultured on coverslips in 6-well plates and fixed in 4% paraformaldehyde for 15 min. DNA strand breaks were identified by TUNEL assay using the KLENOW FragEL™ DNA fragmentation detection kit (Calbiochem, cat no. QIA21) following the manufacturer's protocol. The cells were counter stained with methyl green. Negative controls were processed identically except that TdT was not added. The incidence of apoptosis was derived from the quotient of apoptotic nucleus number divided by the sum of total cell numbers in each coverslip. All measurements were performed by one person.

Detection of poly-(ADP-ribose) polymerase (PARP) cleavage

Cells were suspended in 300 μL of lysis buffer (20 mM HEPES, pH 7.9; 0.2% 0.1% Triton X-100; 10% glycerol; 0.1 mM EDTA; 200 mM NaCl; 1 mM DTT; 0.1 M PMSF; 0.5 μg/mL leupeptin, 0.5 μg aprotinin; Refs. 10, 11). After sonication, the lysate was cleared by centrifugation for 10 min at 12,000 g. Ten micrograms of protein was resolved by 7.5% SDS-PAGE after incubation for 15 min at 65°C. Then, membrane was incubated with anti-PARP (C-2-10; 1:1000, Zymed Laboratory, Inc., San Francisco, CA, cat no. 33-3100) in 5% nonfat dry milk/TBS-t for 1 h and then anti-mouse IgG (1:5000, Transduction Laboratory, cat. no. 15345) for 1 h. The molecular weight of intact PARP and cleaved PARP were 116 KDa and 85 KDa, respectively.

Western blotting analysis of Bcl-xL

Four volumes of extraction buffer (20 mM Tris-HCl, pH 7.4; 2 mM EDTA; 2 mM EGTA; 0.1 mM PMSF; 10 μg/mL aprotonin; 10 μg/mL leupeptin; 10 mM NaF; 6 mM mercaptoethanol; 1% Triton X-100; 0.1% SDS, 10 mM NaCl) was added to the sample and homogenized by sonication (12). The suspension was subsequently centrifuged for 80 min at 16000 g and the clear lysate was ready for protein concentration analysis. Five micrograms of protein was separated by 12.5% SDS-PAGE. Blots were then incubated with Bcl-xL antibody (1:1000, monoclonal; Transduction Laboratory, cat no. B61220, Lexington, KY) in TBS-t containing 5% nonfat milk and then incubated with goat antimouse IgG (1:5000, HRP conjugated, Transduction Laboratory, cat no. M15345). Immunoreactive proteins were visualized by enhanced chemiluminescence.

Construction of PKCα antisense expression vector and transfection

The total RNA from rat liver was isolated using TRIzol reagent (Life Technologies, Grand Island, NY). First-strand cDNA was synthesized using reverse transcription polymerase chain reaction (RT-PCR) kit (Promega, Madison WI). PCR was performed using a Perkin-Elmer thermocycler (Model 2400) for 35 cycles. The forward primer 5′-CCC AAG CTT CAG CTG GTC ATC GCT AAC AT-3′ and reverse primer 5′-GGA ATT CGA TCA CTT ATG GAC TAA TAT CC-3′ for rat PKCα were used in PCR with modifications by adding a *Hind*III site and a *Eco*RI site at 5′ end of the forward and reverse primers, respectively. An amplification program of denaturation (95°C, 1 min), annealing (55°C, 1 min), and extension (72°C, 2 min) was used. A 264-bp PKCα cDNA fragment obtained from PCR amplification was ligated into the TA cloning vector (Invitrogen, San Diego, CA). DNA sequencing was performed to confirm the sequence of the insert. A 254-bp fragment was released from TA cloning vector by digesting with *Hind*III and *Eco*RI. After digestion, the fragment was purified from an agarose gel and then inserted into pcDNA3.1(−)/neo expression vector (Promega) in an antisense orientation named as pAS-PKCα (13).

Clone-9 cells were washed with wash medium (Gibco) and plated onto poly-L-lysine-coated culture well in attachment medium. After 3 h, the medium was changed to DMEM containing 5% fetal calf serum, 1×10^{-8} M dexamethasone, 10 ng/mL epidermal growth factor, 5 μg/mL insulin, 2.5 μg/mL fungizone, 50 μg/mL gentamycin, 67 μg/mL penicillin, and 100 μg/mL streptomycin. Cells were cultured in their usual, serum-containing medium until they reached 80% confluency. The cells were then washed twice with Opti-MEM I reduced-serum medium, and transfected with 2 μg of plasmid DNA/2 mL culture well using 10 μL of Lipofectamin. In each experiment, 1 μg of a green fluorescent protein (GFP) vector (Promega) was co-transfected as a transfection marker. After transfection, the cells were incubated in reduced-serum medium for 8 h then replaced with normal growth medium and immunofluorescence was detected 72 h later.

Immunofluorescence

Cells were fixed with 4% (w/v) paraformadehyde for 15 min and incubated for 1 h at room temperature with primary antibody of PKCα (1:100, Transduction Laboratory), Bcl-xL Ab (1:50, Transduction Laboratory), or antibody recognizing PARP 85-kDa fragment (1:100 dilution, Promega, cat no. G7341) in phosphate-buffered saline (PBS) containing 5% bovine serum albumin. After washing with PBS, cells were incubated for 1 h with secondary antibody-conjugated Texas red (1: 50, ICN Pharmaceuticals, Inc., cat no. 55544). Finally, cells were mounted with PBS containing 80% glycerol and observed for green or red fluorescence using a fluorescent microscope. Ten fields were examined in each sample. Green fluorescence of GFP was used as a transfection marker and red fluorescence after immunostaining of PARP or TUNEL identified an apoptotic-positive cell. However, cells exhibiting GFP fluorescence but not red fluorescence after PKCα or Bcl-xL immunostaining were identified as by suppressed by PKCα or down-regulated by of Bcl-xL, respectively.

Statistics

The statistical analysis of the data was performed by using the one-tailed Student *t* test. A 95% confidence limit was accepted as statistically significant.

RESULTS

Suppression of PKCα by transient antisense treatment

The efficiency of PKCα antisense in suppressing the PKCα protein expression was confirmed by Western blot analysis. Both the protein expressions of the cytosolic and membrane-associated fractions of PKCα were significantly ($P < 0.01$) decreased by 36% and 34%, respectively, after treatment of PKCα-antisense (Fig. 1).

Effect of PKCα antisense treatment on the cell viability, PARP cleavage, and apoptosis

PKCα antisense treatment for 6 h resulted in a significant decrease ($P < 0.01$) of cell count (Fig. 2a). The PARP cleavage from a 116-kDa protein to 85-kDa fragment was detected by Western blot analysis using antibody recognizing both the cleavage and intact PARP. A 100.8% increase of PARP cleavage ($P < 0.01$) was observed after treatment of PKCα-antisense (Fig. 2b). Furthermore, TUNEL stain was performed to detect nuclear DNA strand breaks. The result showed that TUNEL positive cells were significantly ($P < 0.01$) increased after PKCα-antisense treatment (Fig. 2c and d).

Effect of PKCα antisense treatment on protein expression of Bcl-xL

To understand the response of Bcl-xL to PKCα suppression, protein expression of Bcl-xL was detected by Western blot

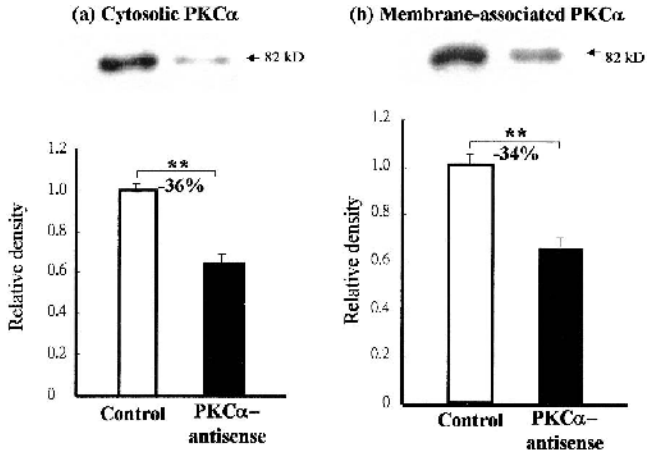

FIG. 1. **Protein expression of PKCα in clone 9 cells treated with or without PKCα antisense.** (a) cytosolic fraction, (b) membrane-associated fraction. Cells were incubated with 1 μM PKCα-antisense for 6 h and samples were collected at 18 h after treatment and then were fractionated into cytosolic and membrane-associated fractions 18 h later. The molecular weight of PKCα is 86 kDa. The data shown indicates mean ±SD of six samples in each group. $^{**}P < 0.01$.

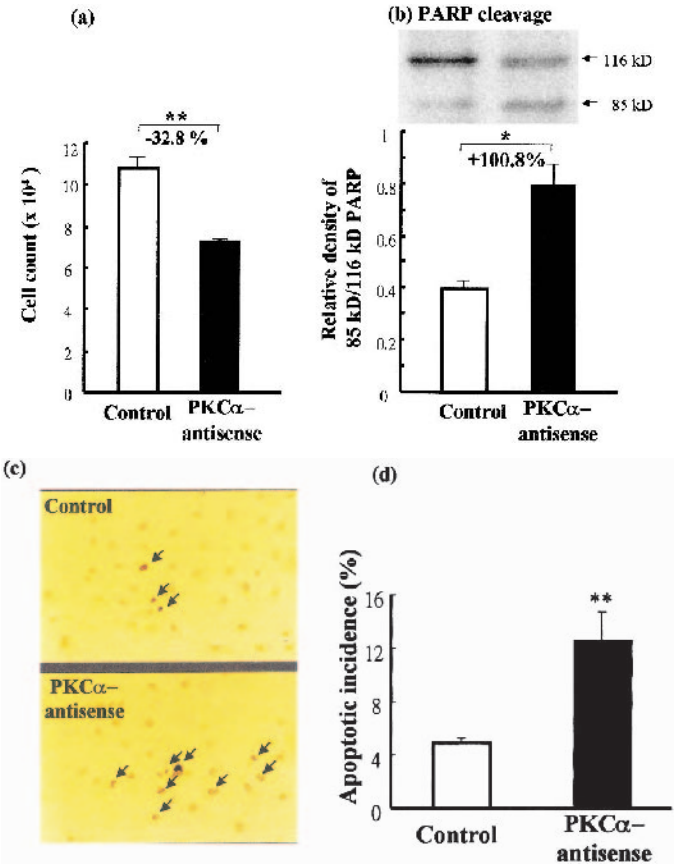

FIG. 2. **Effects of PKCα antisense treatment on (a) cell viability, (b) PARP cleavage, (c) apoptosis, and (d) quantitative apoptotic incidence.** Cells were incubated with 1 μM PKCα-antisense for 6 h and then replaced with fresh medium. Cell viability, PARP cleavage, and apoptotic incidence were evaluated at 18 h after replacement. Cell viability was determined by trypan blue exclusion test. PARP cleavage was detected by immunostaining with Ab against both 116-kDa PARP and 85-kDa fragment of PARP. Apoptotic cells showed in (c) was identified by TUNEL staining. Arrow indicates cell with apoptotic nucleus. The quantitative data of apoptotic incidence was derived from the quotient of apoptotic nucleus divided by the sum of total cell number. The data shown indicates mean ± SD of six samples in each group. $^{**}P < 0.01$.

analysis. Result showed that the expression of anti-apoptotic Bcl-xL protein was significantly ($P < 0.01$) decreased by 32% after PKCα-antisense treatment (Fig. 3).

Suppression of PKCα by transfection with vector containing PKCα cDNA in antisense orientation (pAS-PKCα)

To confirm the long-lasting suppression of PKCα expression by antisense transfection, the protein expression of PKCα was detected by immunostaining with antibody conjugated with Texas red at 72 h after transfection. Cells showing green fluorescence represented as a successful transfection marker. The result showed that after pAS-PKCα transfection, most of the cells expressing GFP (Fig. 4, upper right panel) revealed significantly ($P < 0.01$) lower level of PKCα protein content (Fig. 4, lower right panel) compared with that of the vector control transfection (Fig. 4, lower left panel).

Effect of pAS-PKCα transfection on apoptosis

Apoptotic cells were evaluated by tetramethyl-rhodamine labeling of DNA break to identify if DNA strand breaks

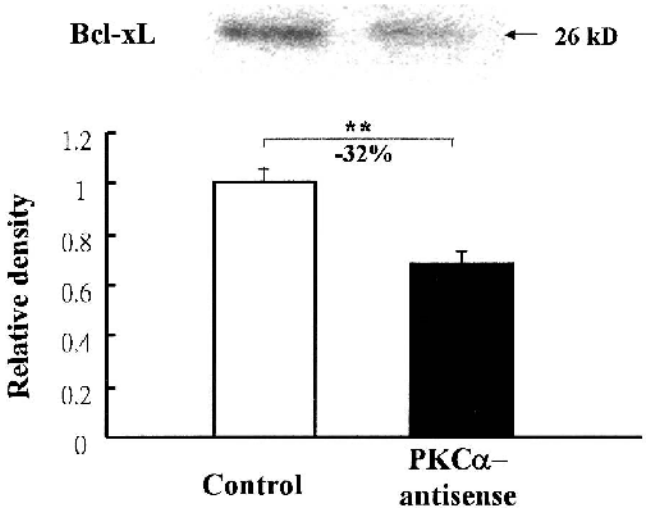

FIG. 3. **Protein expression of Bcl-xL with of without PKCα antisense.** Cells were treated with 1 μM PKCα antisense for 6 h and sampled at 18 h after fresh medium replacement for immunoblotting. The molecular weight of Bcl-xL is 26 kDa. The data shown indicate means ± SD of sixe samples in each group. $^{**}P < 0.01$.

occurred *in situ* after successfully transfected with pAS-PKCα. The result showed that the percentage of both GFP expression and TUNEL staining double-positive cells after pAS-PKCα transfection was significantly ($P < 0.01$) higher than that of vector control transfection (Fig. 5).

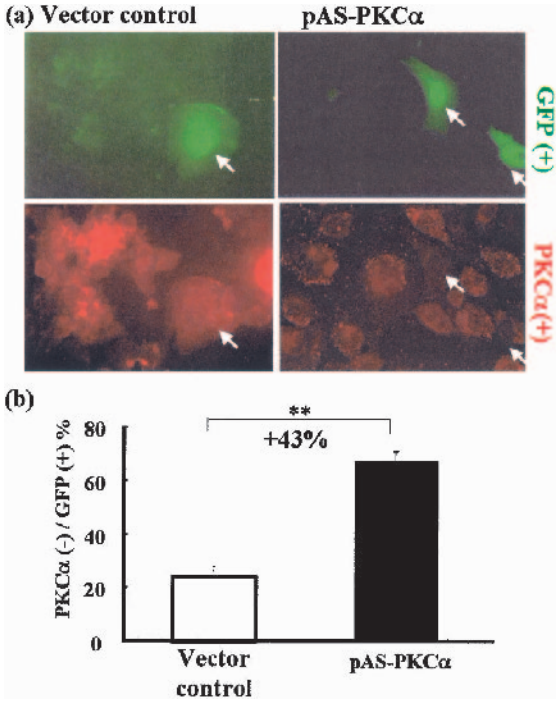

FIG. 4. **Decrease of PKCα protein expression after transfection with vector containing PKCα antisense (pAS-PKCα).** (a) Immunofluorescent image of GFP expression (upper panel) and PKCα immunoreactive (lower panel) cells. (b) Quantitative ratio of PKCα negative-expression cells per GFP (+) cells. Cells transfected with vector control and pAS-PKCα was showed in left and right panel, respectively. Green fluorescence represented as a transfection marker. Red fluorescence indicates PKCα immunoreactive cells, which was stained with antibody conjugated with Texas red. Arrow indicates the relative PKCα reactivity in the cell, which is simultaneously GFP (+). The percentages of PKCα negative whereas GFP (+) cells were presented as means ±SD of 5 samples in each group. $^{**}P < 0.01$.

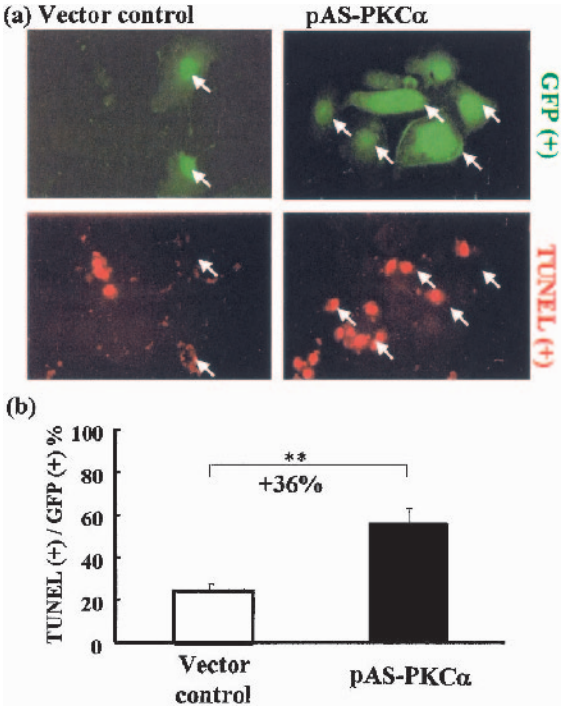

FIG. 5. **Increase of apoptotic incidence after transfecting with vector containing PKCα cDNA in antisense orientation (pAS-PKCα).** (a) Immunofluorescent image of GFP expression (+) (upper panel) and TUNEL stain (+) (lower panel) cells. (b) Quantitative ratio of TUNEL (+) cells per GFP (+) cells. Cells transfected with vector control and pAS-PKCα was showed in left and right panel, respectively. GFP cDNA was co-transfected as a transfection marker. Red fluorescence indicates apoptotic cells, which were evaluated by tetramethyl-rhodamine labeling of DNA break. Arrow indicates the DNA strand breaks in the cells, which is simultaneously GFP (+). The percentages of double-positive cells were presented as mean ± SD of five samples in each group. $^{**}P < 0.01$.

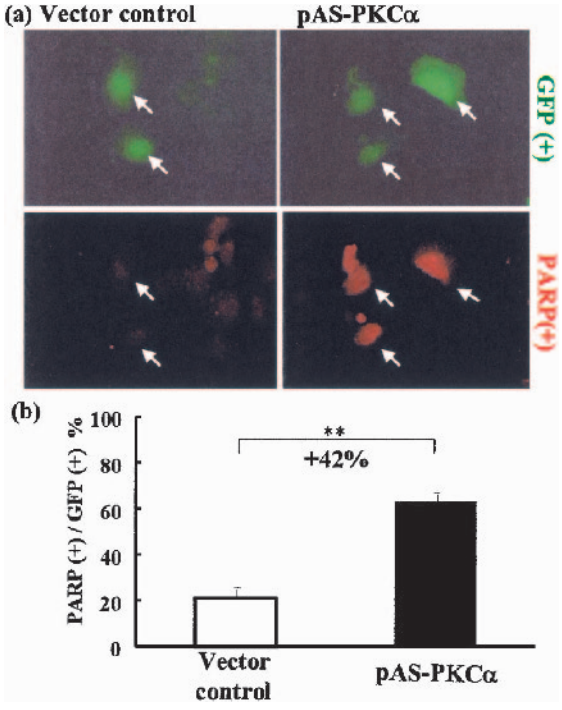

FIG. 6. **Increase of the PRAP cleavage after transfecting with vector containing PKCα cDNA in antisense orientation (pAS-PKCα).** (a) Immunofluorescent image of GFP expression (+) (upper panel) and 85kD PARP immunoreactive (lower panel) cells. (b) Quantitative ratio of PARP (+) cells per GFP (+) cells. Cells transfected with vector control and pAS-PKCα was showed in left and right panel, respectively. GFP cDNA was co-transfected as a transfection marker. Red fluorescence indicates the cleaved PARP 85 kDa, which was detected by immunostaining with 85-kDa PARP antibody conjugated with Texas red. Arrow indicates the relative PARP cleavage in the cell, which is simultaneously GFP (+). The percentages of double-positive cells were presented as mean ± SD of five samples in each group. $^{**}P < 0.01$.

PARP cleavage induced by transfection with pAS-PKCα

To further understanding the possible pathways of apoptosis triggered by PKCα suppression, the caspase-dependent cleavage of PARP was detected by immunostaining with antibody recognizing only the 85-kDa fragment of PARP conjugated with Texas red after pAS-PKCα transfection. The result showed that the percentage of cells expressing GFP associated with PARP cleavage after pAS-PKCα transfection was significantly ($P < 0.01$) higher than that of vector control transfection (Fig. 6).

Effect of pAS-PKCα transfection on Bcl-xL immunoreactivity

The expression of Bcl-xL, which affects cytochrome C release and caspase activation, was detected after pAS-PKCα transfection by immunostaining with antibody conjugated with Texas red. Green fluorescence was also used as a transfection marker. The result showed that, after pAS-PKCα transfection, the percentage of cells expressing GFP concomitant with a negative expression of Bcl-xL protein was significantly ($P < 0.01$) higher than those of vector control transfection as showed in Figure 7.

DISCUSSION

The present study provided evidence that suppression of PKCα by antisense increased the apoptotic incidence in hepatic epithelial cell line. Furthermore, *in situ* down-regulation of Bcl-xL, PARP cleavage, and DNA strand breaks occurred when the cell was successively transfected with pAS-PKCα. It suggests that PKCα plays a critical role in cell survival and the expression of the cell survival molecule, Bcl-xL, is modulated by the PKCα signaling pathway.

The liver is essential in regulating host defenses to septic challenge and the degree of hepatic failure during sepsis is related to the extent of cell damage and death resulting from either necrosis or apoptosis. Although hepatic apoptosis has been reported to be a less apparent phenomenon during sepsis in some previous reports (14, 15), induction of apoptosis correlated with a reduced Bcl-2 content had been reported in endotoxin-treated animals (16). Our previous results showed that hepatic apoptosis was apparently increased at early sepsis and persisted to the late stage of sepsis whether it was evaluated by flow cytometry, PARP cleavage, TUNEL stain or even by the less sensitive DNA ladder gel electrophoresis. Because of the rapid turnover of apoptotic cells by Kupffer cell, the prolonged and constant hepatic apoptosis might contribute to hepatic failure during polymicrobial sepsis.

It is well documented that PKC inhibitor is an effective apoptotic-inducing agent. Previous report indicated that calphostin, a specific PKC inhibitor, induced apoptosis associated with down-regulation of Bcl-xL as well as activation of caspase-3 (17). However, the role of each isoform of PKC in

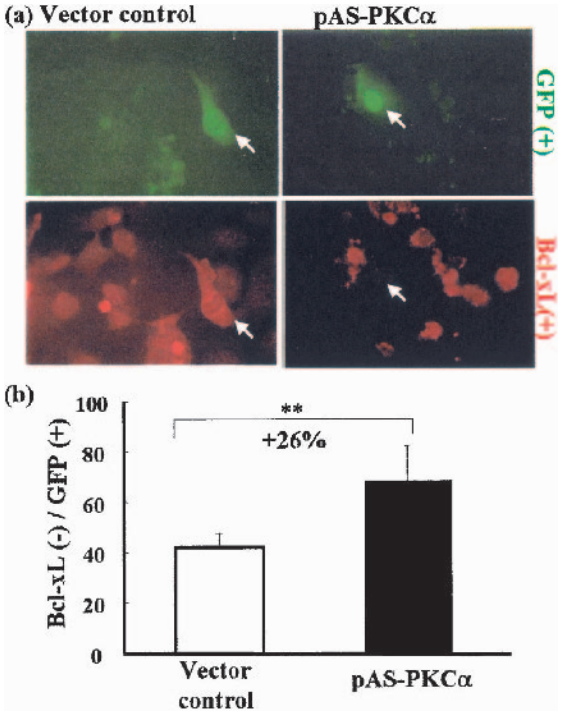

FIG. 7. **Decrease of Bcl-xL protein expression after transfecting with vector containing PKCα cDNA in antisense orientation (pAS-PKCα).** (a) Immunofluorescent image of GFP expression (+) (upper panel) and Bcl-xL immunoreactive (lower panel) cells. (b) Quantitative ratio of Bcl-xL negative-expression cells per GFP (+) cells. Cells transfected with vector control and pAS-PKCα was showed in left and right panel, respectively. GFP cDNA was co-transfected as a transfection marker. Red fluorescence indicates Bcl-xL immunoreactive cells, which was stained by antibody conjugated with Texas red. Arrow indicates the relative immunoreactivity of Bcl-xL in the cells, which is simultaneously GFP (+). The percentages of Bcl-xL negative whereas GFP (+) cells were presented as mean ± SD of five samples in each group. $^{**}P < 0.01$.

apoptosis is not identified. Previous studies have demonstrated that loss of PKCα function correlated with the induction of apoptosis in COS cells (18). Inhibition of PKCα gene expression by ribozyme also resulted in a significant apoptosis in glioma cells through suppressing Bcl-xL gene expression (3). Although treatment with phorbol 12-myristate 13-acetate (TPA), PKC activator, upregulated expression of Bcl-xL in human erythropoietin-dependent cell line (19). Our previous report showed that, during sepsis, inactivation of PKCα was accompanied by reduction in Bcl-xL levels that coincided with the appearance of apoptotic cell death in liver (5). The present result showed that the protein content of Bcl-xL was significantly decreased by *in situ* PKCα suppression. It strongly supports a potential interaction between PKCα and the Bcl-xL protein. Recently, our preliminary result showed that the expression of Bcl-xL mRNA under PKCα suppression was also decreased (unpublished data). It suggests that PKCα may modulate the transcriptional regulation of Bcl-xL. However, the molecular mechanism involved in apoptosis triggered by PKCα suppression need further study. In addition, a previous study showed that over-expression of PKCα resulted in increased mitochondrial PKCα localization and Bcl-2 phosphorylation, which is required for antiapoptotic function (20). Therefore, the expression of the apoptosis-related proteins in addition to Bcl-xL may be modulated by PKCα suppression. In this respect, comparison analysis between control and stably PKCα-antisense transfected cells by the PCR-based differential display technique identified some genes, which are under investigation in our laboratory.

The immunohistochemical results of our previous study showed that, during sepsis, PKCα was significantly decreased especially within the nucleus (2). It is possible that the declination of nuclear PKCα might regulate the expression of apoptosis-related protein, i.e., Bcl-xL, through modulating the phosphorylation/dephosphorylation state of transcriptional factors. Transcriptional factors, i.e., Ets, nuclear factor-κB, STAT, and activator protein-1, play essential roles in determining the fate of a cell by affecting the expression of bcl-x gene encoding the anti-apoptotic Bcl-xL protein (21). Several hypotheses offer potential mechanisms how Bcl-xL exerts its survival effects. Previous reports implicated that Bcl-xL promotes cell survival by regulating the electrical and osmotic homeostasis of mitochondria (22). Besides, Bcl-xL functions as a facilitator of ADP supply to the mitochondrial matrix, allowing for continued F1F0-ATPase activity (23). If the mitochondrial respiration terminates through loss of F1F0-ATPase activity, mitochondria will release cytochrome C, which induce apoptopsome formation and subsequent caspase activation associated with endonucleosomal PARP cleavage and apoptosis. Previous study showed that Bcl-xL prevents the staurosporin-induced apoptosis of dopaminergic neurons by inhibiting the caspase activation (24), which is a subsequent process after damage of the outer mitochondrial membrane and cytochrome c release. In addition, the bulk of the bcl-xL product localizes to the periphery of mitochondria (25). Bcl-xL may also function as, or association with, a mitochondria ion channel to regulate apoptosis (22, 26). It can also close the voltage-dependent anion channel preventing cytochrome c to pass through the channel (27). Taken together, these observations suggest that mitochondria may play a crucial role in Bcl-xL regulated apoptosis caused by PKCα suppression. Further evaluation of the causal relationship between PKCα and mitochondrial function will be performed in the near future.

In conclusion, the present results indicated that suppression of PKCα decreased the cellular contents of Bcl-xL and leaded to a caspase-dependent apoptosis in hepatic epithelial cells. Therefore, PKCα may be a therapeutic target for prevention of apoptosis during sepsis.

REFERENCES

1. Hsu C, Jao HC, Yang SL, Hsu HK, Liu MS: Inactivation of protein kinase C in rat liver during late hypoglycemic phase of sepsis. *Mol Cell Biochem* 181:181–189, 1998.
2. Hsu C, Hsieh YC, Hsu HK, Jao SC, Yang RC: Alteration of protein kinase C isoforms in the liver of septic rat. *Shock* 17:41–46, 2002.
3. Leirdal M, Sioud M: Ribozyme inhibition of the protein kinase C alpha triggers apoptosis in glioma cells. *Br J Cancer* 80:1558–1564, 1999.
4. Capiati DA, Vazquez G, Tellez Inon MT, Boland RL: Antisense oligonucleotides targeted against protein kinase c alpha inhibit proliferation of cultured avian myoblasts. *Cell Prolif* 33:307–315, 2000.
5. Jao HC, Yang RC, Hsu HK, Hsu C: The decrease of PKCalpha is associated with hepatic apoptosis at early and late phases of polymicrobial sepsis. *Shock* 15:130–134, 2001.
6. Dean NM, McKay R, Condon TP, Bennett CF: Inhibition of protein kinase C-alpha expression in human A549 cells by antisense oligonucleotides inhibits

induction of intercellular adhesion molecule 1 (ICAM-1) mRNA by phorbol esters. *J Biol Chem* 269:16416–16424, 1994.
7. Baxter GT, Miller DL, Kuo RC, Wada HG, Owicki JC: PKC epsilon is involved in granulocyte-macrophage colony-stimulating factor signal transduction: evidence from microphysiometry and antisense oligonucleotide experiments. *Biochemistry* 31:10950–10954, 1992.
8. Wise BC, Glass DB, Chou CH, Raynor RL, Katoh N, Schatzman RC, Turner RS, Kibler RF, Kuo JF: Phospholipid-sensitive Ca^{2+}-dependent protein kinase from heart. II. Substrate specificity and inhibition by various agents. *J Biol Chem* 257:8489–8495, 1982.
9. Ways DK, Cook PP, Webster C, Parker PJ: Effect of phorbol esters on protein kinase C-zeta. *J Biol Chem* 267:4799–4805, 1992.
10. Desnoyers S, Shah GM, Brochu G, Poirier GG: Erasable blot of poly(ADP-ribose) polymerase. *Anal Biochem* 218:470–473, 1994.
11. Keppler-Hafkemeyer A, Brinkmann U, Pastan I: Role of caspases in immunotoxin-induced apoptosis of cancer cells. *Biochemistry* 37:16934–16942, 1998.
12. Arber N, Han EK, Sgambato A, Piazza GA, Delohery TM, Begemann M, Weghorst CM, Kim NH, Pamukcu R, Ahnen DJ, Reed JC, Weinstein IB, Holt PR: A K-ras oncogene increases resistance to sulindac-induced apoptosis in rat enterocytes. *Gastroenterology* 113:1892–1900, 1997.
13. Zhang X, Wen J, Aletta JM, Rubin RP: Inhibition of expression of PKC-alpha by antisense mRNA is associated with diminished cell growth and inhibition of amylase secretion by AR4-2J cells. *Exp Cell Res* 233:225–231, 1997.
14. Hiramatsu M, Hotchkiss RS, Karl IE, Buchman TG: Cecal ligation and puncture (CLP) induces apoptosis in thymus, spleen, lung, and gut by an endotoxin and TNF-independent pathway. *Shock* 7:247–253, 1997.
15. Hotchkiss RS, Swanson PE, Cobb JP, Jacobson A, Buchman TG, Karl IE: Apoptosis in lymphoid and parenchymal cells during sepsis: findings in normal and T- and B-cell-deficient mice. *Crit Care Med* 25:1298–1307, 1997.
16. Haendeler J, Messmer UK, Brune B, Neugebauer E, Dimmeler S: Endotoxic shock leads to apoptosis in vivo and reduces Bcl-2. *Shock* 6:405–409, 1996.
17. Ozaki I, Tani E, Ikemoto H, Kitagawa H, Fujikawa H: Activation of stress-activated protein kinase/c-Jun NH2-terminal kinase and p38 kinase in calphostin C-induced apoptosis requires caspase-3-like proteases but is dispensable for cell death. *J Biol Chem* 274:5310–5317, 1999.
18. Whelan RD, Parker PJ: Loss of protein kinase C function induces an apoptotic response. *Oncogene* 16:1939–1944, 1998.
19. Tsushima H, Urata Y, Miyazaki Y, Fuchigami K, Kuriyama K, Kondo T, Tomonaga M: Human erythropoietin receptor increases GATA-2 and Bcl-xL by a protein kinase C-dependent pathway in human erythropoietin-dependent cell line AS-E2. *Cell Growth Differ* 8:1317–1328, 1997.
20. Ruvolo PP, Deng X, Carr BK, May WS: A functional role for mitochondrial protein kinase Calpha in Bcl2 phosphorylation and suppression of apoptosis. *J Biol Chem* 273:25436–25442, 1998.
21. Sevilla L, Zaldumbide A, Pognonec P, Boulukos KE: Transcriptional regulation of the bcl-x gene encoding the anti-apoptotic Bcl-xL protein by Ets, Rel/NFkappaB, STAT and AP1 transcription factor families. *Histol Histopathol* 16:595–601, 2001.
22. Vander Heiden MG, Chandel NS, Williamson EK, Schumacker PT, Thompson CB: Bcl-xL regulates the membrane potential and volume homeostasis of mitochondria. *Cell* 91:627–637, 1997.
23. Vander Heiden MG, Chandel NS, Schumacker PT, Thompson CB: Bcl-xL prevents cell death following growth factor withdrawal by facilitating mitochondrial ATP/ADP exchange. *Mol Cell* 3:159–167, 1999.
24. Kim JE, Oh JH, Choi WS, Chang II, Sohn S, Krajewski S, Reed JC, O'Malley KL, Oh YJ: Sequential cleavage of poly(ADP-ribose)polymerase and appearance of a small Bax-immunoreactive protein are blocked by Bcl-X(L) and caspase inhibitors during staurosporine-induced dopaminergic neuronal apoptosis. *J Neurochem* 72:2456–2463, 1999.
25. Gonzalez-Garcia M, Perez-Ballestero R, Ding L, Duan L, Boise LH, Thompson CB, Nunez G: bcl-XL is the major bcl-x mRNA form expressed during murine development and its product localizes to mitochondria. *Development* 120:3033–3042, 1994.
26. Muchmore SW, Sattler M, Liang H, Meadows RP, Harlan JE, Yoon HS, Nettesheim D, Chang BS, Thompson CB, Wong SL, Ng SL, Fesik SW: X-ray and NMR structure of human Bcl-xL, an inhibitor of programmed cell death. *Nature* 381:335–341, 1996.
27. Shimizu S, Shinohara Y, Tsujimoto Y: Bax and Bcl-xL independently regulate apoptotic changes of yeast mitochondria that require VDAC but not adenine nucleotide translocator. *Oncogene* 19:4309–4318, 2000.